Histol Histopathol (2011) 26: 979-995

http://www.hh.um.es

Histology and Histopathology

Cellular and Molecular Biology

Phenotypic changes and possible angiogenic roles of pericytes during wound healing in the mouse skin

Shunichi Morikawa and Taichi Ezaki

Department of Anatomy and Developmental Biology, School of Medicine, Tokyo Women's Medical University, Tokyo, Japan

Summary. Pericytes (PCs) are attracting increasing attention as a crucial target for anti-angiogenic therapy. In this study, we sought to determine the functional significance of PCs during angiogenesis by using a skin wound healing model in which different angiogenic stages are identifiable. Angiogenesis was first observed on Day 3 after wounding and increased greatly on Day 5. On Day 5, the leading edge of the regenerating vessels (vascular advancing front; VAF) appeared to be composed of immature vessels, and was further divided into "tip" and "following" regions according to maturational differences. PCs distributed in regenerating vessels showed phenotypic differences according to different regions. PCs that expressed PDGFR-ß alone and lacked vascular basement membrane (BM) were predominant in the tip region of the VAF, while PCs that expressed both PDGFR-ß and NG2 with their BM coating were numerous in the following regions toward the rear of the VAF. Moreover, PCs in the VAF expressed VEGF-A and associated with most proliferating endothelial cells (ECs). VEGF-A expression of PCs and the proliferating ECs totally disappeared in the region toward the rear of the VAF. We conclude that PCs can differ in their phenotype according to the stage of angiogenesis during wound healing. They may promote angiogenesis at the initial stage but might in turn stabilize the newly formed vessels at the later stage.

Key words: Pericytes, Angiogenesis, Wound healing, VEGF-A, Endotel

Offprint requests to: S. Morikawa, Department of Anatomy and Developmental Biology, Tokyo Women's Medical University, 8-1 Kawada-cho, Shinjuku, Tokyo 162-8666, Japan. e-mail: shun@research.twmu.ac.jp

Introduction

Pericytes (PCs) are found on the abluminal surface of endothelial cells (ECs) of microvessels, and are usually covered with a vascular basement membrane (BM), in common with the ECs (Diaz-Flores et al., 1991, 2009; Sims, 2000; Armulik et al., 2005). However, in special cases, they are located outside the BM and are thus situated not in an "intramural" but in an "extramural" position (Ashton and de Oliveira, 1966; Nehls and Drenckhahn, 1993). Unlike vascular smooth muscle cells in arterioles and larger venules that are distributed densely around the vessels and show a regular circumferential orientation, PCs are usually distributed sparsely on vessels and show a rather longitudinal orientation of their cell bodies (Diaz-Flores et al., 1991, 2009; Morikawa et al., 2002).

Among their functional roles, such as the regulation of microvascular blood flow (Diaz-Flores et al., 1991, 2009; Sims, 2000), their role in angiogenesis is of great importance at present, since increasing attention has been focused on these cells as a possible target of anti-angiogenic therapy in various diseases which are dependent on angiogenesis, such as tumors (Erber et al., 2004; Baluk et al., 2005; Sennino et al., 2007, 2009). Inhibition of EC proliferation and stabilization of the vessel wall (Orlidge and D'Amore, 1987; Sato and Rifkin, 1989; von Tell et al., 2006) have long been suggested as functions of PCs in angiogenesis. However, some authors have proposed that PCs are able to induce EC proliferation and guide EC sprouts during angiogenesis (Rhodin and Fujita, 1989; Schlingemann et al., 1991; Nehls et al., 1992; Wesseling et al., 1995; Reynolds and Redmer, 1998; Amselgruber et al., 1999; Reynolds et al., 2000; Morikawa et al., 2002; Ozerdem and Stallcup, 2003).

We hypothesized that these conflicting theories might reflect heterogeneity of PCs at the different stages

(initial or later maturing stage) of angiogenesis. Providing evidence of our hypothesis would be of great importance for comprehensive understanding of angiogenic mechanisms, and for developing effective clinical anti-angiogenic therapies that target PCs. In this study, we sought to determine whether PCs differ in their phenotypes and functional roles based on the different stages of angiogenesis using multiple morphological approaches. To achieve this aim, we employed a mouse skin wound model in which blood vessels regenerate orthodromically toward the central region of defected tissue. This property enabled us to specify the different stages of angiogenesis. Vessels located at the leading edge of the regenerating vascular network should be the youngest or in the initial stage of angiogenesis, while vessels located in the rear should be in the maturing stage.

Using this wound model, we first examined the time course of angiogenesis during wound healing to judge the most suitable time point for detailed study of angiogenesis. We then specified the vascular advancing front (VAF) of the regenerating blood vessels to observe the initial stage of angiogenesis. PCs were then immunohistochemically identified in situ with specific PC markers PDGFR-ß and NG2, both of which especially well depict nascent PCs (Hellstrom et al., 1999; Bergers and Song, 2005; Hall, 2006), and their distribution, phenotypic characteristics, VEGF-A expression, association with proliferating ECs, and vascular BM coating were examined by confocal laser scanning microscopy. Finally, we performed a detailed examination with semi-thin or ultrathin sections to further characterize the PCs in the initial stage of angiogenesis, and compared these with those in the maturing stage, based on their association with EC sprouts, vascular BM coating, and intracellular specializations at the ultrastructural level.

Materials and methods

Animals

Male BALB/c mice (8-10 weeks old) were purchased from SLC Inc. (Shizuoka, Japan) and maintained in air-filtered clean rooms at the Institute of Laboratory Animals, Tokyo Women's Medical University; the mice were fed with sterilized standard laboratory chow and provided with water ad libitum. All experiments were conducted in accordance with legislation of the Institute of Laboratory Animals at Tokyo Women's Medical University. Intramuscular injection of ketamine (87 mg/kg) plus xylazine (13 mg/kg) was used to anesthetize the mice throughout the experiments.

Manipulation for experimental wound models

Under anesthesia, the dorsal flanks of the mice were shaved and circular wounds that extended to the depth of the superficial fascia were made with a 2-mm diameter skin punch (Fray Products Corp., Buffalo, NY; Fig. 1A). Wounds were allowed to heal after they were covered with a sheet of sterile gauze. After wounding, animals were carefully monitored twice a day to ensure that the wounds did not become infected and that the animals were not in pain.

BrdU labeling of proliferating cells

Three mice were injected intraperitonealy with a thymidine analogue, 5- bromo-2'-deoxy-uridine (BrdU; Sigma-Aldrich, St. Louis, MO, USA, 1 mg in 100 μl of PBS per mouse) 3 h prior to fixation for labeling of proliferating cell nuclei. The dose of BrdU and the labeling time were chosen for the distinct labeling of proliferating ECs according to our previous work (Ezaki et al., 2001).

Intravital blood vessel labeling with tomato lectin

On days 1, 3, 5, and 10 after wounding, three mice were injected with 50 μl of fluorescein isothiocyanate (FITC)-labeled tomato lectin (*Lycopersicon esculentum* lectin: 1 mg/ml; Vector Laboratories, Burlingame, CA), into the femoral vein under anesthesia to enable visualization of the blood vessels by lectin binding. Injected lectin was allowed to circulate in the vasculature for 10 min. After circulating the lectin, the chest of the animals was opened and the vasculature was perfused from the left ventricle with 100 ml of 2% paraformaldehyde (PFA) in 0.01 M phosphate-buffered saline (PBS: pH 7.4) at a pressure of 120 mmHg. The wound tissues were then removed together with the surrounding skin and soaked in the same fixative at 4°C for 30 min. The wound tissues were then washed with PBS, mounted on glass slides, and examined as whole-mount preparations.

Tissue preparation for immunohistochemistry

Wound tissues (some perfused with lectin) obtained on Day 5 after wounding were perfusion-fixed as described above. After post-fixation and PBS washing, the wound tissues were immersed in PBS containing a graded series of sucrose (10, 15, and 30%) at 4°C, embedded in Tissue-Tek OCT compound (Sakura Finetek, Torrance, CA, USA), and snap-frozen in liquid nitrogen. Cryostat sections were made and further processed for immunohistochemistry.

Immunohistochemistry

Frozen sections were first incubated in 4% Block Ace (Dainippon Seiyaku, Osaka, Japan) to block nonspecific immunoreactions, and successively incubated with primary antibodies (alone or in combination) in PBS containing 1% bovine serum albumin (Sigma, St Louis, MO, USA) at 4°C overnight.

PCs were identified with antibodies to platelet-derived growth factor-ß (PDGFR-ß: a rat monoclonal, clone APB5, 1:100 (e-Biosciences, San Diego, CA, USA), NG2 chondroitin sulfate proteoglycan (a rabbit polyclonal 1:500; Chemicon, Billerica, MA, USA), Alpha-smooth muscle actin (α-SMA; Cy3-conjugated mouse monoclonal, clone1A4, 1:500; Sigma-Aldrich, Saint Louis, MO, USA) and desmin (a rabbit polyclonal, 1:200, Abcam, Cambridge, MA, USA). ECs were identified with antibodies to CD31 [a rat monoclonal (clone MEC 13.3, 1:250; BD Pharmingen, San Diego, CA, USA), or a hamster monoclonal (clone 2H8, 1:400; Chemicon), or a rabbit polyclonal (1:200; Spring Bioscience, Pleasanton, CA, USA)]. Vascular endothelial growth factor-A (VEGF-A) expressing cells were marked with a goat polyclonal antibody to mouse VEGF-A, (1:100; R&D Systems, MN, USA). Basement membrane was identified with antibodies against type IV collagen (a rabbit polyclonal 1:1000; Cosmo Bio, Tokyo, Japan). After several washes with PBS, specimens were incubated with combinations of fluorescent (FITC, TRITC, and Cy5) conjugated anti-rat, -hamster, -goat and -rabbit secondary antibodies (Jackson ImmunoResearch, West Grove, PA, USA) for 3 h at room temperature. To visualize BrdU incorporation in proliferating cell nuclei, sections were immunostained first with the markers for PCs and ECs, and then incubated with biotinylated mouse anti-BrdU antibody (1:10; BD Pharmingen). The biotinylated antibodies were then visualized with Cy5 conjugated streptavidin (1:200; Jackson ImmunoResearch). Immunostained sections were examined with a Leica TCS-SL confocal laser-scanning microscope (Leica Microsystems, Wetzlar, Germany). For observation, we used 10x dry (Plan Fluotar, NA: 0.30), 20x dry (Plan Apo, NA: 0.70), and 63x water immersion (Plan Apo, NA: 1.20) objective lenses. Confocal images were captured at 512x512 pixels (8 bit), scan speed of 400 Hz, and a pinhole determined according to the size of the Airy disk.

Transmission electron microscopy

Anesthetized mice were fixed by vascular perfusion of 4% PFA and 2.5% glutaraldehyde in 0.1M sodium cacodylate buffer (100ml; pH 7.4) at a pressure of 120 mmHg. Immediately after the perfusion, the wound regions were removed, cut into small pieces, and immersed in the same fixative for another 2 h at 4°C. Specimens were then treated with 1% osmium tetroxide for 2 h at 4°C, and then with saturated uranyl acetate for 3 h at room temperature. Thereafter, specimens were dehydrated in a graded series of ethanol and embedded in epoxy resin. Semi-thin sections 0.5 μm in thickness were made from the resin- embedded specimens and counterstained with toluidine blue for light microscopy. For photographing the semi-thin sections, 100x oil immersion objective lens (UPlan SApo, NA: 1.40) was used. After making the semi-thin sections, ultrathin sections 70 nm in thickness were made, counterstained with saturated uranyl acetate followed by lead citrate, and observed with a Hitachi H-7000 electron microscope (Hitachi, High-Technologies Co., Tokyo, Japan).

Quantitative analysis

Using the sections stained with PDGFR-ß, CD31,

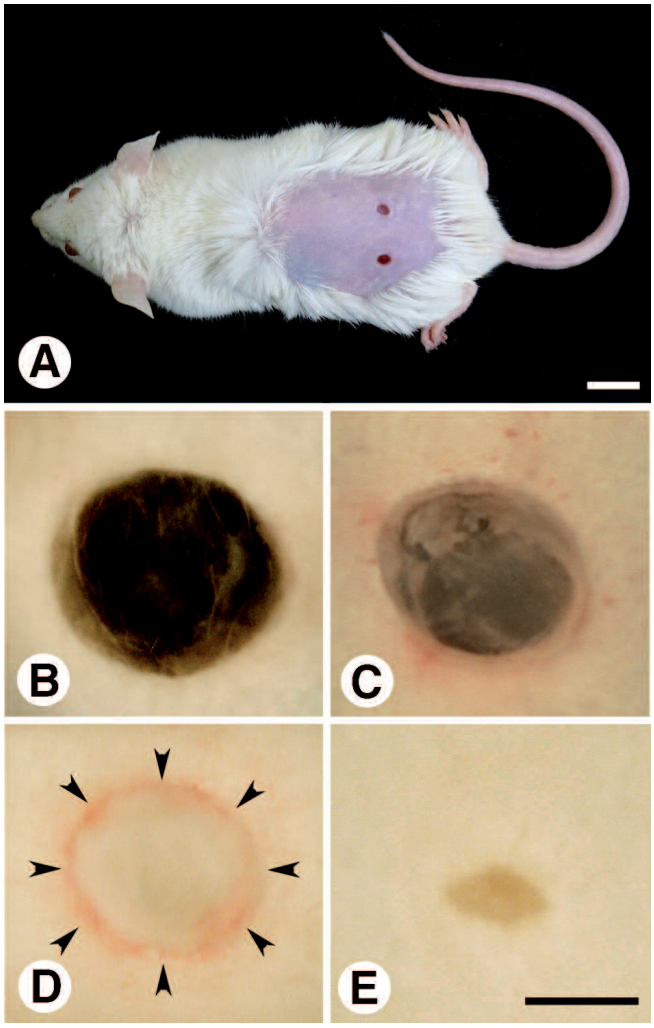

Fig. 1. Time course of wound healing in the mouse skin. **A.** A mouse immediately after wounding. Two circular wounds of about 2 mm in diameter that extended to the superficial fascia were made on the skin of the dorsal flanks. (**B–E):** Overview of wound whole-mount preparations 1, 3, 5, and 10 days after wounding. View from the inner surface of the wounds. **B.** On Day 1, the appearance of the wounds was essentially the same as when they were made. No obvious changes were visible at the macroscopic level. **C.** On Day 3, the boundary of the wound narrowed and the surface of the wound was covered with a thin coating of regenerated epithelia. **D.** On Day 5, regenerated epithelia became thickened and a blood-containing circle at the wound boundary caused by hemorrhage was clearly visible (arrowheads). **E.** On Day 10, the blood-containing circle had disappeared and the surface area of the wound was greatly reduced in comparison to that of the Day 5 wound. Scale bar: A, 1 cm; B-E, 1 μm.

and BrdU, 150-μm square areas in the tip and following regions of the VAF were identified with confocal microscopy (n=3 animals). Subsequently, the number of proliferating ECs and their association with PCs was determined and the mean ratio of ECs with PC association was calculated. The values indicated in Table 1 are expressed as mean ± SEM (standard error of the mean).

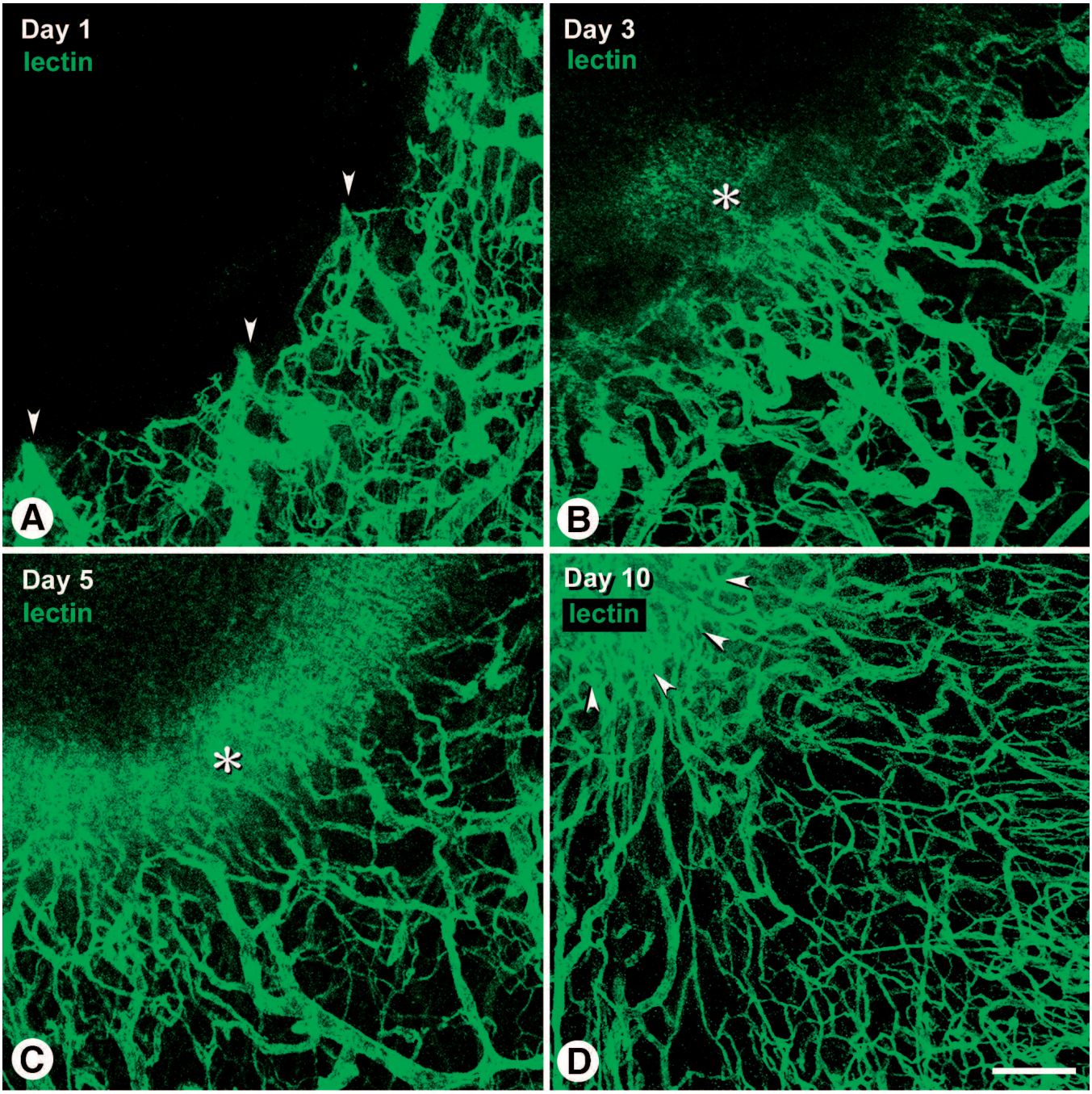

Fig. 2. Time course of angiogenesis in mouse skin wounds visualized by lectin perfusion. Blood vessels were visualized by intravenously injected FITC-conjugated tomato lectin in whole-mount preparations of skins on Day 1 **(A)**, Day 3 **(B)**, Day 5 **(C)**, and Day 10 **(D)**. **A.** On Day 1, the edges of the wounded vessels are clearly visible (arrowheads) and no extravasation of perfused lectin is observed. **B.** On Day 3, lectin leakage (asterisk) from regenerating vessels become visible at the anterior area of the regenerating vessels. **C.** On Day 5, the whole vascular network narrows toward the center of the wound. At the same time, lectin leakage is more conspicuous (asterisk) and forms a circular structure at the anterior region of the regenerating vessels. **D**. On Day 10, the wounded region is completely vascularized by regenerated vessels. A small amount of extravasated lectin is still noticeable at the center of the wound (arrowheads). Magnifications are the same in all figures. Scale bar: 200 μm.

Results

Time course of angiogenesis during wound healing

The time course of the macroscopic wound healing process at 1, 3, 5, and 10 days after wounding is shown in Fig. 1. On the first day after wounding, the blood vessel network surrounding the wounded area was clearly demarcated microscopically by binding of intravenously perfused tomato lectin, and the cut ends of

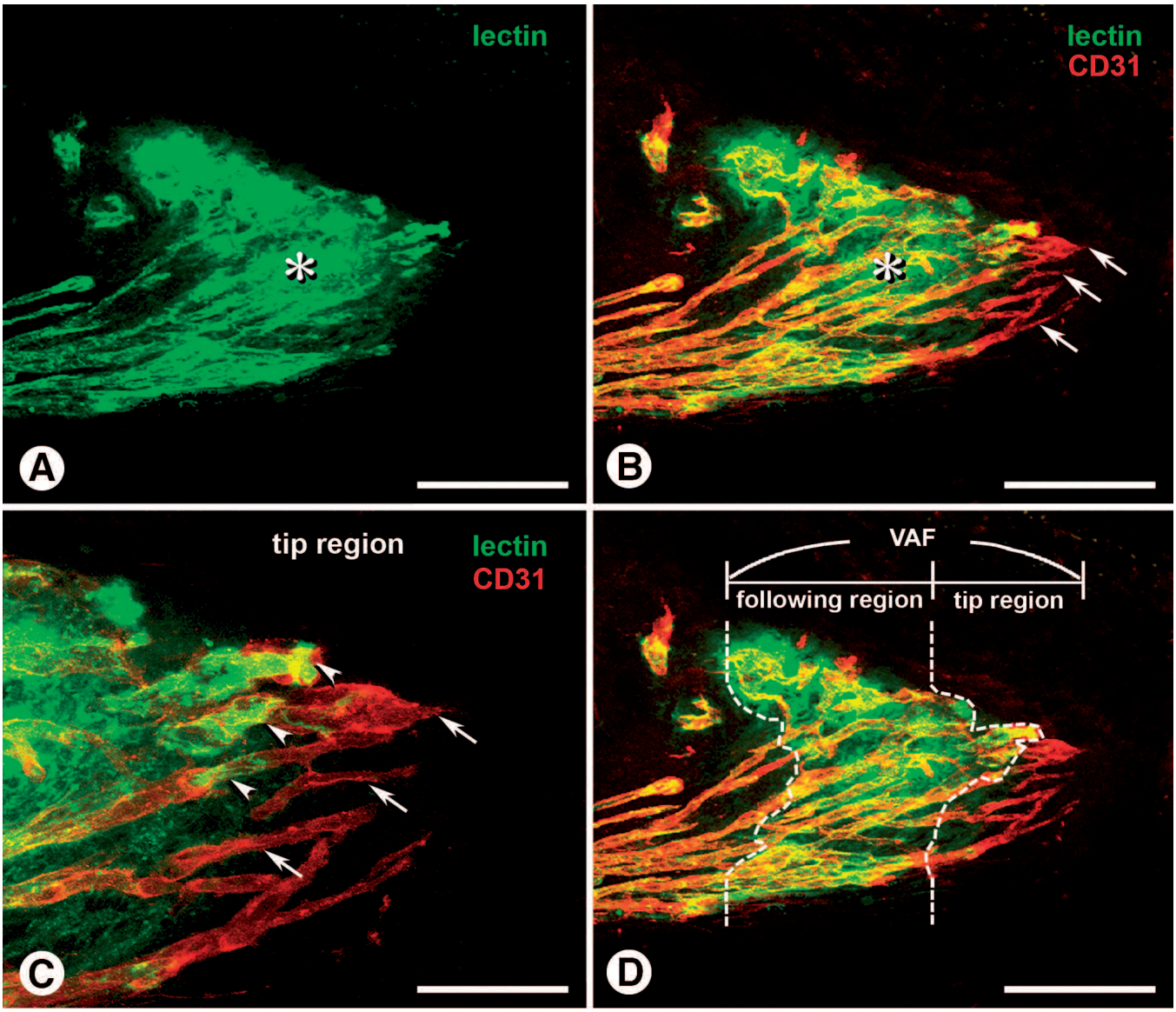

Fig. 3. Identification of the vascular advancing front (VAF) of regenerating vessels. **A.** A vertical section of a Day 5 wound that was intravenously injected with tomato lectin. Regenerating vessels are stained with perfused lectin, yet extravasation of the lectin (asterisk) is prominent in the anterior region. **B.** The same region as **A**. When CD31 immunostaining is applied to the section, CD31 immunoreactivity is found in vessels intraluminally stained with lectin, including those in the area accompanied by lectin leakage (asterisk). However, at the same time, CD31 also reveals CD31+ ECs lacking intraluminal lectin staining beyond the vessels with lectin leakage (arrows). **C.** Higher magnification of the foremost area shown in B. Lectin-inaccessible vessels (lectin-/CD31+; arrows) are located beyond the lectin-accessible but leaky vessels (lectin+/CD31+; arrowheads). **D.** Same micrograph as B. Judging from the observations, the anterior region of the regenerating vessels appeared to be composed of immature vessels. This region was able to be further divided into two regions based on the accessibility of perfused lectin: the tip region is the foremost region where the lectin-inaccessible vessels are distributed, and following region is the region behind the tip where the lectin accessible but leaky vessels are located. We designated the total region combining these two as the vascular advancing front (VAF). The ranges of the tip and following regions are not constant in the vascular network (dotted lines) due to differences in individual vessel lengths. We estimated that lectin-/CD31+ vessels and lectin+/CD31+ leaky vessels were generally about 150 μm and 200 μm in width, respectively, in the vascular networks of the Day 5 specimens examined. For convenience, we therefore roughly delimited the ranges of the tip and following regions in the entire regenerating vascular network to be of 150 μm and 200 width, respectively. Scale bar: A, B, D, 150 μm; C, 55 μm.

vessels were also clearly visible (Fig. 2A). On Day 3, regenerating vessels penetrated toward the wound center. Thus the whole wounded area was reduced in comparison to that of Day 1 (Fig. 2B). At the same time, extravasated lectin spread over the anterior region of the regenerating vessels was also identified and was presumably elicited by the increased permeability of newly formed ECs during the angiogenic process. On

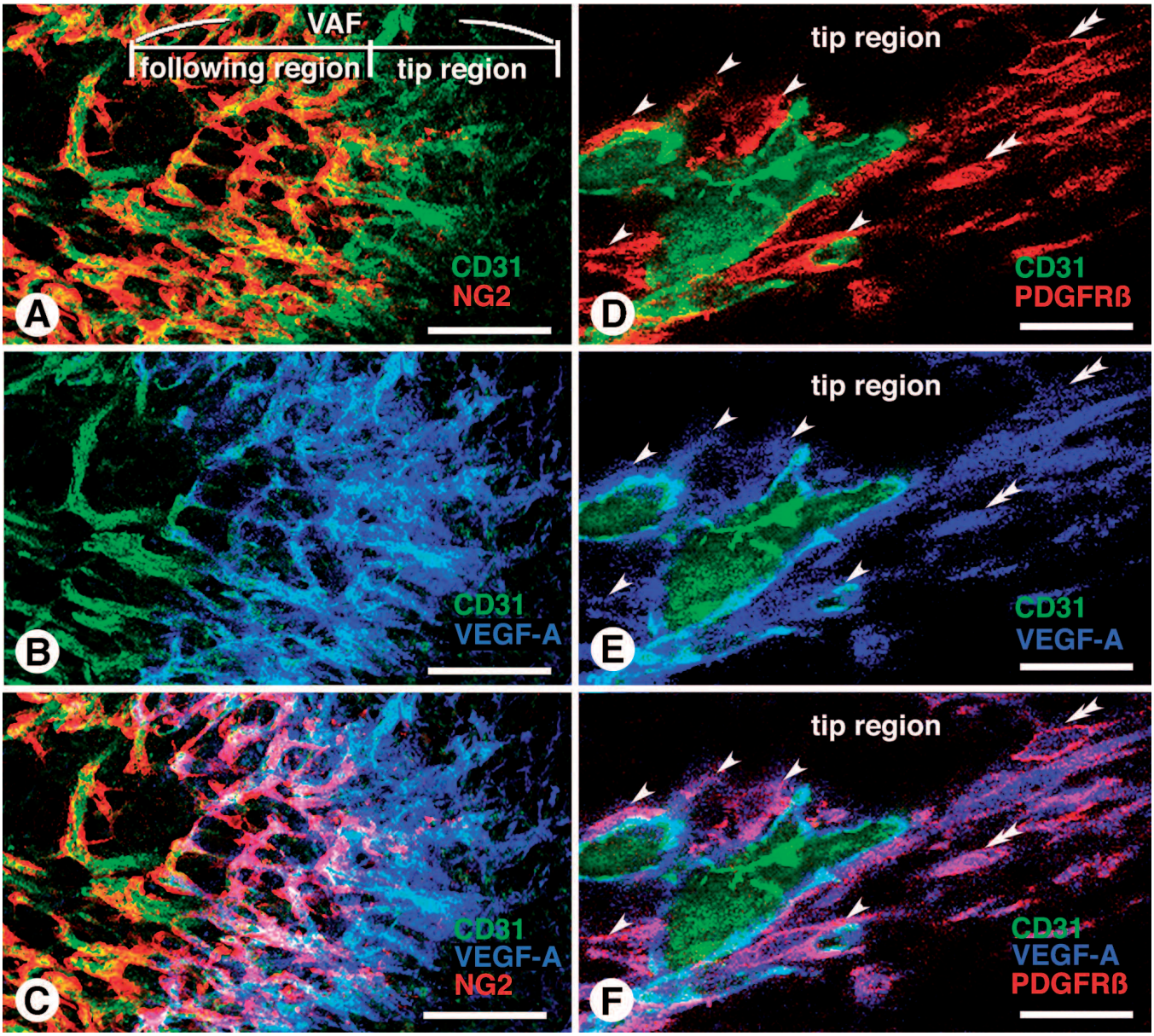

Fig. 4. PC distribution and VEGF-A expression in the regenerating vessels of a Day 5 wound. **(A-C)**: Vessels were stained with NG2, CD31, and VEGF-A. **A.** NG2+ PCs are distributed abundantly throughout the regenerating vessels except for at the tip region of VAF, where they are only sparsely distributed. **B.** Same region as A. VEGF-A is expressed intensely within the confines of VAF. **C.** Merged image of A and B. NG2+ PCs (red) located in the tip region and the anterior portion of the following region of VAF express VEGF-A (blue) and were thus stained light purple, while NG2+ PCs located in the rear of VAF do not express VEGF-A, and are thus stained red alone. The ranges of the tip and following regions are delimited with reference to those of the lectin-perfused specimens. Magnifications are the same in A–C. Bar length in C: 75 μm. **(D–F)**: The tip region of VAF stained with PDGFR-ß, CD31, and VEGF-A. **D.** Contrary to the NG2 staining, PDGFR-ß+ PCs are abundant in the tip region of VAF. **E.** Same region as **D** showing VEGF-A expression around the vessels in the tip region. **F.** Merged image of D and E. Light purple staining of PCs indicates co-localization of PDGFR-ß (red) and VEGF-A (blue) in the PCs (arrowheads). Concurrent expression of PDGFR-ß and VEGF-A is also observed in stromal cells that are not in contact with ECs. These stromal cells show a spindle-shaped, fibroblast-like morphology (D–F: double arrowheads). Scale bar: 25 μm.

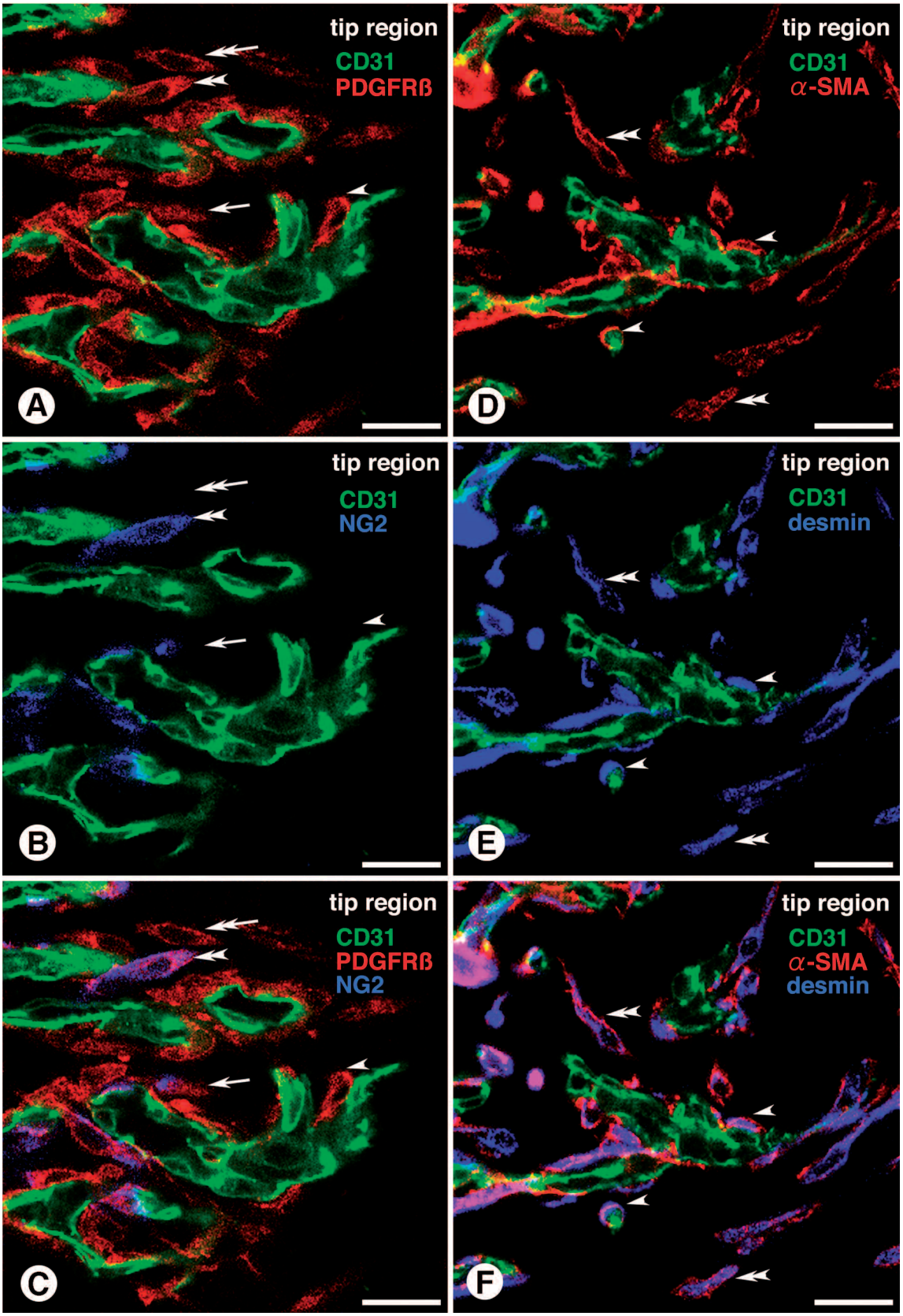

Fig. 5. Different marker expression by PCs in the tip region of VAF in a Day 5 wound. Micrographs (**A-C**) and (**D-F**) show the same regions, respectively. (**A-C**): PCs were visualized with a combination of PDGFR-ß and NG2. **A.** PDGFR-ß+ PCs are consistently distributed in VAF. **B.** Same region as **A**. NG2+ PCs are unevenly distributed and tend to be absent in the tip of VAF. **C.** When images **A** and **B** are merged, it becomes apparent that PCs that express PDGFR-ß alone are found in the first half of the tip region in particular (arrowhead); PCs double positive for PDGFR-ß and NG2 are gradually intermingled in the latter half of the region (double arrowhead). Note that PCs show uniform expression of PDGFR-ß but partial expression of NG2 (arrow). In the tip region, PDGFR-ß+/NG2-stromal cells that are out of contact with ECs are also observed (**A-C**: arrow with double arrowheads). (**D-F**): PCs were visualized with a combination of α-SMA and desmin. **D.** PCs in VAF express α-SMA (arrowheads), while stromal cells that are not in contact with ECs also positive for α-SMA (double arrowheads). **E.** Same region as **D**. Similar to the α-SMA, desmin is expressed not only by PCs (arrowheads), but also stromal cells (double arrowheads). **F.** Merged image of **D** and **E**. Scale bar: 25 μm.

Day 5, vessels regenerated further and the area encircled by the regenerating vessels became narrower than that on Day 3 (Fig. 2C). Further, the amount of extravasated lectin increased and formed a clear circular structure at the anterior region of the regenerating vessels (Fig. 2C). On Day 10, the whole wounded area was covered with a regenerated vascular network. At the center of the wound, a small amount of lectin leakage was noticeable, suggesting that the angiogenic process was still underway in this small portion of the wound (Fig. 2D).

From the observations above, we chose the Day 5 wound for more detailed examination, since lectin extravasation was most conspicuous at this time point, and the large amount of lectin leakage was considered to reflect increased angiogenic activity.

Organization of the vascular advancing front (VAF) in regenerating vessels

When CD31 immunostaining was performed on the sections of lectin-perfused Day 5 wound tissues, it became apparent that the CD31+ vessels that were intraluminally marked with lectin were distributed across the areas of leaked lectin (Fig. 3A-C). Moreover, the presence of lectin-unstained CD31+ vessels was also apparent (Fig. 3B,C). These lectin-inaccessible vessels were located beyond the lectin-accessible vessels (Fig. 3B,C); they represent the foremost point of the regenerating vessels, an area that perfused lectin had not been able to access due to their lack of luminal surfaces (Morikawa et al., 2002).

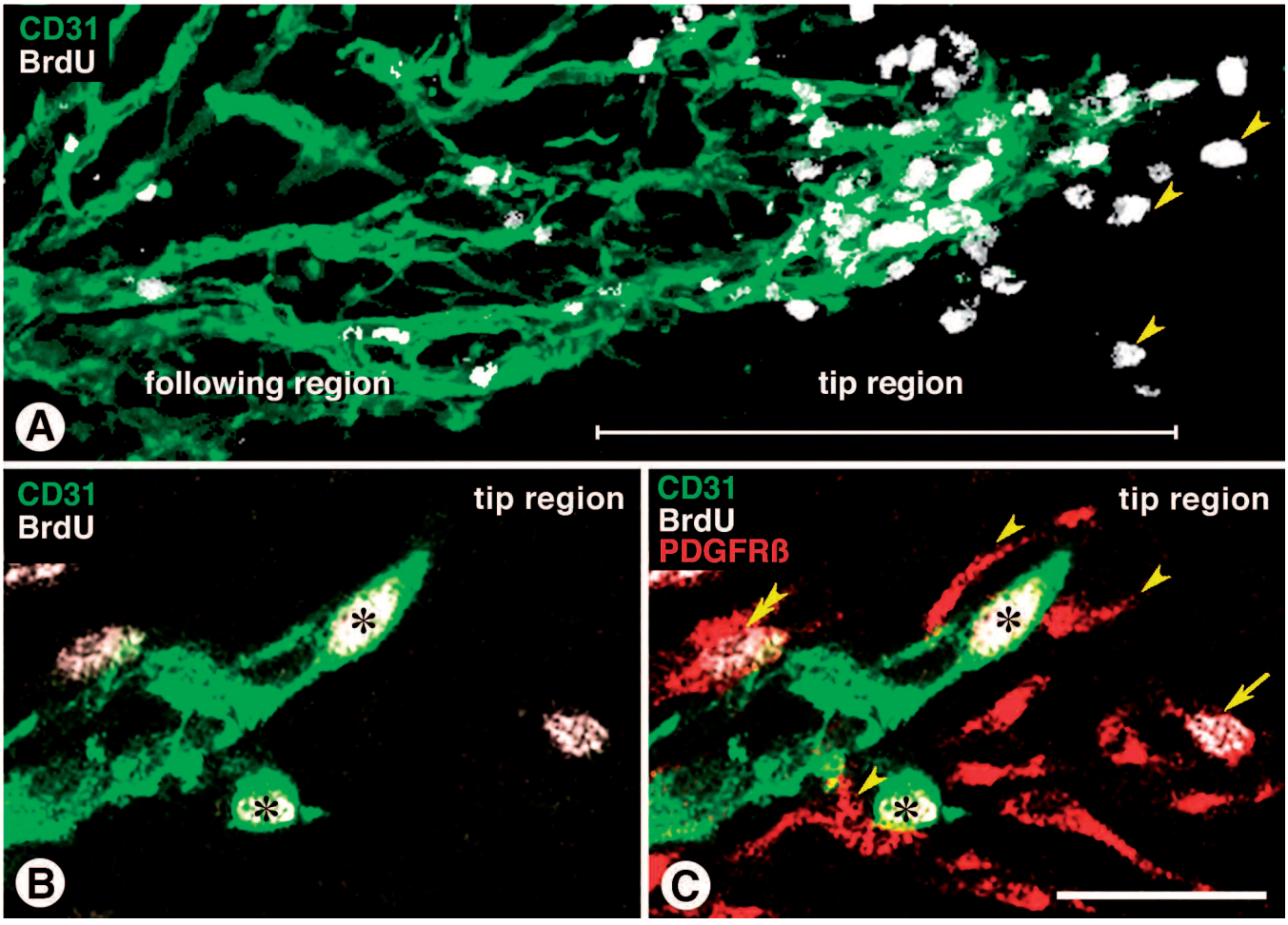

Fig. 6. Association of PCs with proliferating ECs in VAF of a Day 5 wound. **A:** CD31+ ECs with BrdU-incorporated proliferative nuclei (white in color) are identified throughout VAF, although they are found to be far more numerous in the tip region than in the following region. Note BrdU+ nuclei located away from ECs (arrowheads). The range of the tip region is delimited with reference to that of lectin-perfused specimens. **B.** Higher magnification of vessels in the tip region showing BrdU+ (asterisks) proliferating ECs. **C.** Same region as **B**. The proliferating ECs (asterisks) are closely associated with PDGFR-ß+ PCs (arrowheads). Note PCs (double arrowheads) and PDGFR-ß+ stromal cells that are out of contact with ECs (arrow) are also proliferating. Scale bar in C applies to all micrographs. Scale bar: A, 55 μm; B, C, 25 μm.

From the observations above, vessels located in the anterior region of the regenerating vascular network were considered to be immature vessels. However, since regional differences in terms of the accessibility of perfused lectin were found between vessels located in this area, we decided to classify these regions before undertaking any further examinations (Fig. 3D). (1) We designated the foremost region, where lectin-inaccessible vessels were distributed, the "tip region" and (2) the region behind the tip region where lectin accessible but leaky vessels were distributed the "following region". (3) Finally, we defined the total region combining these two regions the "vascular advancing front or VAF". Since the lengths of the individual vessels differed, the ranges of the "tip region" and "following region" varied considerably in each vascular network (Fig. 3D; dotted lines). In general, lectin-/CD31+ vessels and lectin+/CD31+ leaky vessels were distributed at a maximum width of about 150 μm and 200 μm, respectively, in the vascular networks of Day 5 specimens examined. For convenience, therefore, we roughly delimited the ranges of the tip and following regions of the regenerating vascular network as having widths of 150 μm and 200 μm, respectively.

Table. 1. Association of PCs with proliferating ECs in the VAF.

	Tip region	Following region
Number of proliferating ECs	21.0±2.5 cells	6.3±2.1 cells
Number of PCs on proliferating ECs	20.7±2.4 cells	6.0±2.0 cells
% of PCs on proliferating ECs	98.6±1.4%	95.2±4.8%

PCs, ECs, and dividing nuclei in the vessels were visualized by PDGFR-ß, CD31, and BrdU immunoreactivities, respectively. The number of proliferating ECs and proliferating ECs with PC association were determined from optical sections of 1 μm thickness obtained with confocal microscopy (image area 150 μm square) and their ratio were calculated (n=3 mice). The values are expressed as means ± SEM.

PC distribution and VEGF-A expression in regenerating vessels

NG2+ PCs were abundantly distributed throughout the regenerating vessels, except at the tip region of the VAF, where they were distributed only sparsely; NG2+ PCs gradually increased in number from the following region toward the rearmost region of VAF (Fig. 4A). When the vessels were stained with VEGF-A, their expression appeared to be limited within the confines of the VAF (Fig. 4B). NG2+ PCs located in the VAF appeared to express VEGF-A; however, their VEGF-A expression disappeared at the rear of the VAF (Fig. 4A-C). In contrast, another PC marker, PDGFR-ß, revealed the presence of abundant PCs (Fig. 4D,F) and their expression of VEGF-A (Fig. 4E,F) in the tip region. In this region, PDGFR-ß+ stromal cells that were not in contact with ECs were identified in the stromal space but these also expressed VEGF-A (Fig. 4D-F). These stromal cells tended to show a spindle-shaped, fibroblast-like morphology (Fig. 4 D-F).

Expression of different markers by PCs in the tip region of the VAF

Differences among PCs in terms of marker expression in the tip region of the VAF were examined in detail. A dual visualization of PCs with a combination of PDGFR-ß and NG2 confirmed that PDGFR-ß+/NG2- PCs were predominant in the tip region (Fig. 5A-C) and, in particular, they were found in the first half of this region exclusively. In contrast, they were gradually seen in combination with PDGFR-ß+/NG2+ PCs in the latter

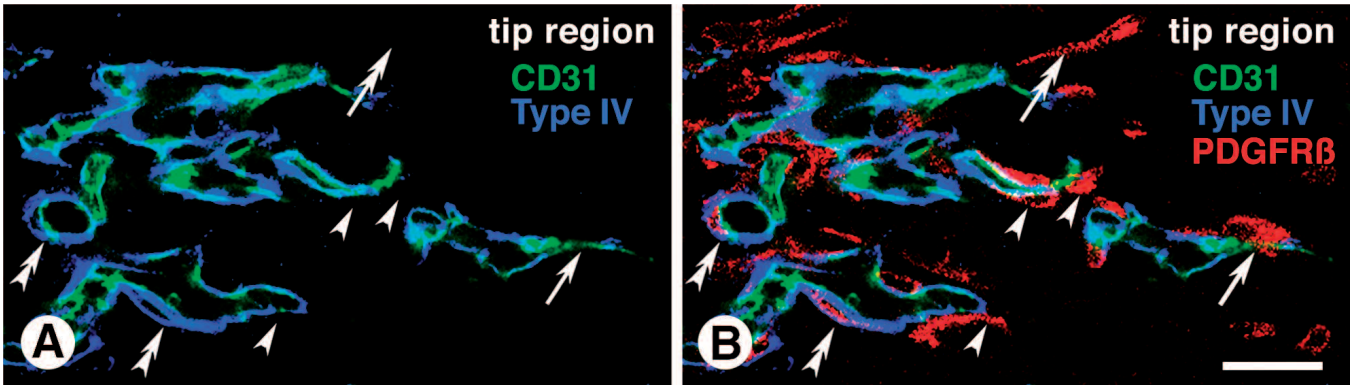

Fig. 7. Different vascular basement membrane (BM) coating of PCs in the tip region of the VAF in a Day 5 wound. **A.** ECs in the tip region of the VAF are enveloped with type IV collagen+ vascular BM on their outer surfaces, although is discontinuous and its coating not complete (arrow) in some portions. **B.** Same region as A. PDGFR-ß+ PCs located in the first half of the tip region typically lack a vascular BM coating (arrowheads), while PCs in the latter half are increasingly covered with a BM in common with the ECs (double arrowheads). Note a PDGFR-ß+ stromal cell that is out of contact with ECs (arrow with double arrowheads) extends a long cytoplasmic process towards EC surfaces. Scale bar: 25 μm.

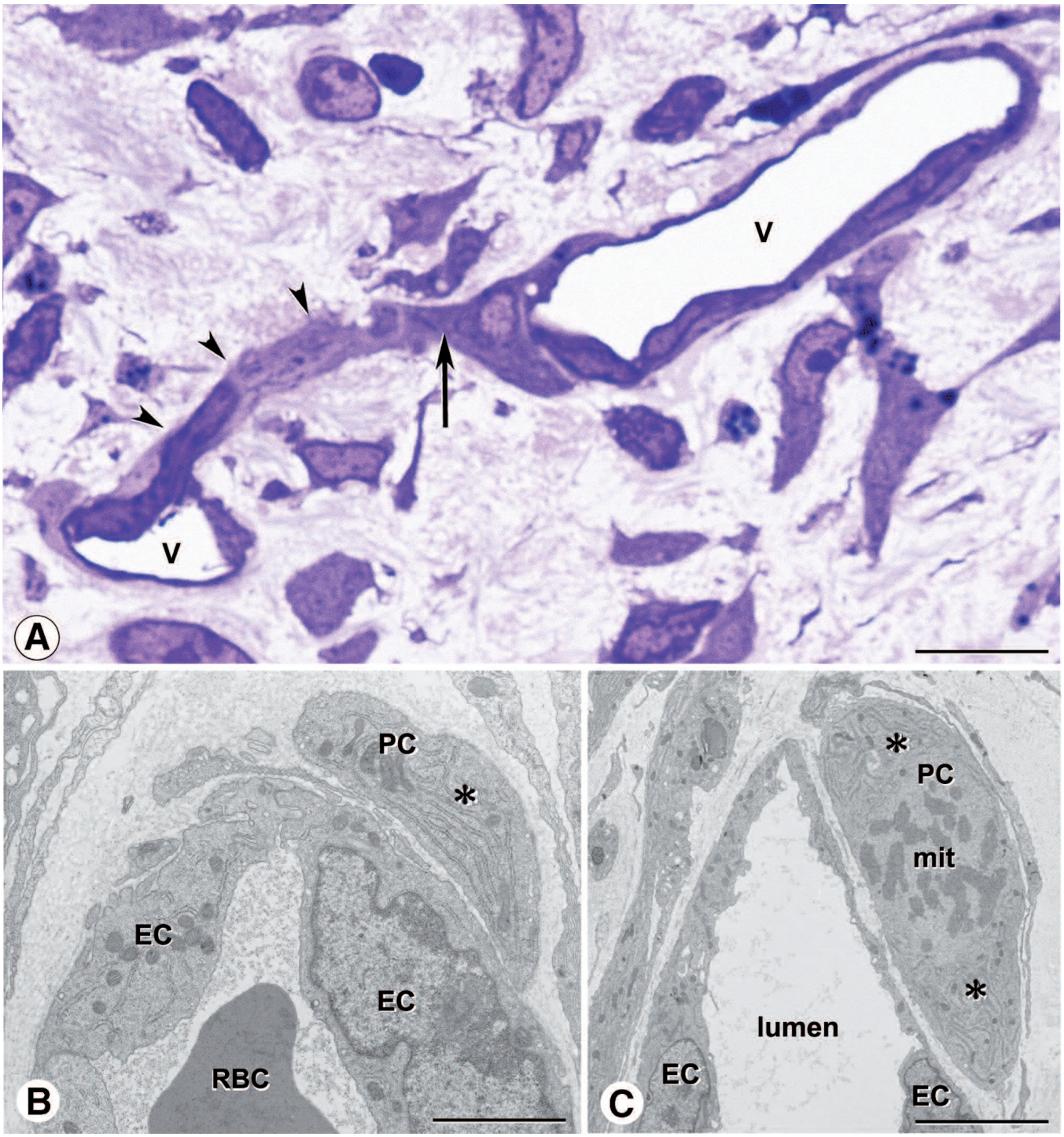

Fig. 8. Semi-thin and ultra-thin sections showing the guidance of a sprouting EC by a PC and ultrastructural features of PCs in the tip region of VAF. **A.** A semi-thin section stained with toluidine blue. A PC (arrow) appears to guide a sprouting EC (arrowheads) to another vessel on which the PC itself is attached. (V): vessels. **B, C**: Electron microscopic images. **B.** A PC on an EC with a well-developed rER (asterisk). RBC: red blood cell. **C.** A PC with a well-developed rER (asterisks) is undergoing mitosis (mit) on an EC. Scale bar: A, 10 μm; B, 2.5 μm; C, 5 μm.

half of the region (Fig. 5B,C). Notably, some PDGFR-ß+/NG2+ PCs in the tip region partially expressed NG2 (Fig. 5B,C), whereas PCs in the following region or in the rear of VAF generally showed a uniform intracellular expression of the two PC markers. Similar to the PCs, stromal cells that were out of contact with ECs also tended to express PDGFR-ß alone (Fig. 5A,C). In addition to PDGFR-ß and NG2, both of which especially well depict nascent PCs in neovascularization, we examined the expression pattern of alpha-smooth muscle actin (α-SMA) and desmin in the PCs of our wound-healing model; these cytoskeletal proteins have also been used to mark PCs in various vascular systems. Consequently, we found that PCs in the VAF expressed both α-SMA and desmin (Fig. 5D-F); moreover, we found that these two markers depicted not only PCs but also stromal cells that were out of contact with ECs (Fig. 5D-F). We also observed that PDGFR-ß expression was co-localized in these α-SMA+/desmin+ stromal cells (data not shown).

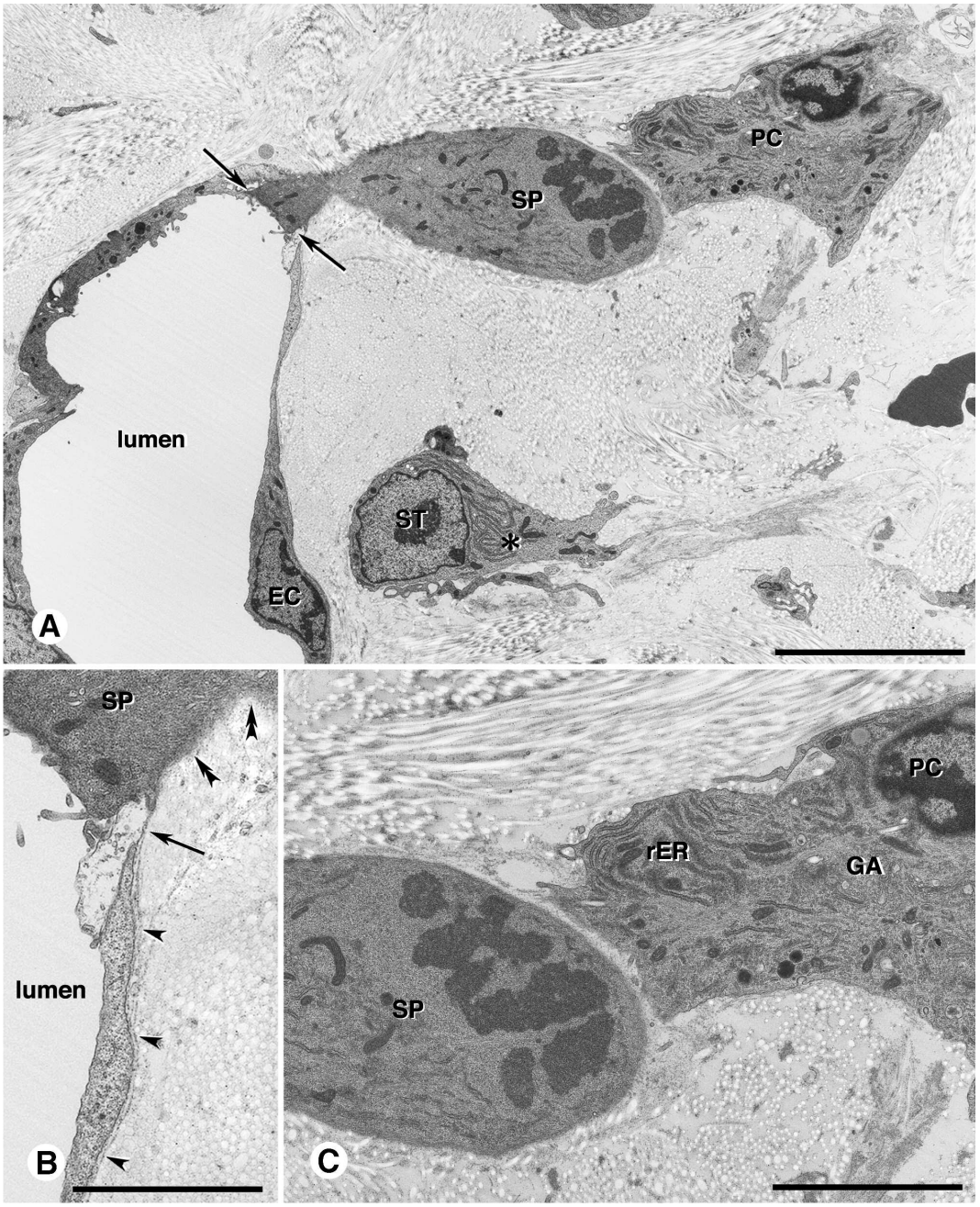

Fig. 9. Electron microscopic image of a PC associated with a newly forming EC sprout in the tip region of VAF. **A.** An EC sprouting from a pre-existing vessel wall (arrows) and extending into the stromal space. The EC sprout (SP) is undergoing mitosis and is closely associated with a PC. Note that this feature corresponds well to those in Fig. 6C. Note a stromal cell (ST) that contains abundant rER (asterisk) is located in close vicinity to the vessel. **B.** Higher magnification of the root of EC sprout shown in **A** (the portion indicated by arrows in A is magnified). The vascular BM that covers the pre-existing vessel wall (arrowheads) disappears at the root of the EC sprout (arrow), resulting in the lack of a BM from the sprout surface (double arrowheads). **C.** Higher magnification of the EC sprout and associating PC shown in **A**. The PC associating with the EC sprout (SP) is characterized by well-developed rER and Golgi apparatus (GA). The surface of the PC is devoid of vascular BM, as is the surface of the associated EC sprout. Scale bar: A, 10 μm; B, C, 4.5 μm.

Association of PCs with proliferating ECs in the VAF

EC proliferation in regenerating vessels was examined using wound specimens to which BrdU was administered. CD31+ ECs with BrdU-incorporated proliferative nuclei were located exclusively in the VAF, although they were found more frequently in the tip than in the following region (Fig. 6A). Proliferating ECs were more than three times as numerous in the tip region as in the following region. Strikingly, regardless of the number of proliferating ECs, almost all proliferating ECs in the whole VAF were closely associated with PDGFR-ß+ PCs (Fig. 6B,C). The ratio of proliferating ECs associated with PCs was more than 98% and 95% in the tip and following region, respectively (Table 1). In addition to the ECs, some PDGFR-ß+ PCs or PDGFR-ß+ stromal cells that were out of contact with ECs proliferated.

Vascular basement membrane (BM) of PCs in the tip region of the VAF

Regenerating vessels were generally covered with vascular BM over their entire surface although BM in the tip region of VAF was discontinuous in some portions (Fig. 7A,B). Remarkably, PDGFR-ß+ PCs located in the first half of the tip region appeared to lack vascular BM; in contrast, PCs in the latter half were increasingly covered with BM in common with the ECs (Fig. 7B). PCs located in the following region and in the rear of VAF also had a continuous vascular BM coating. Further, some PDGFR-ß+ stromal cells that were out of contact with ECs often approached EC surfaces with long slender cytoplasmic processes most likely used for attachment (Fig. 7B).

Ultrastructural features of PCs in the tip region of the VAF

Morphological features of the PCs in the regenerating vessels were further examined with semi-thin and ultra-thin sections. In the VAF, EC sprouts from vessels were often identified, especially in the tip region, while they were absent from the rear of the VAF. Notably, some sprouts appeared to be guided by PCs to other vessels on which the PCs themselves attached (Fig. 8A). At the ultrastructural level, PCs in the tip region of the VAF were characterized by rich cellular organelles, especially well-developed rough endoplasmic reticulum (rER), compared with those in the rear of the VAF (Fig. 8B), suggesting active protein synthesis of the PCs in this region. In addition, some PCs were found to be undergoing mitosis in this region (Fig. 8C).

Furthermore, also in the tip region, EC sprouts undergoing mitosis were identified at the ultrastructural level (Fig. 9). In these areas, PCs were also closely

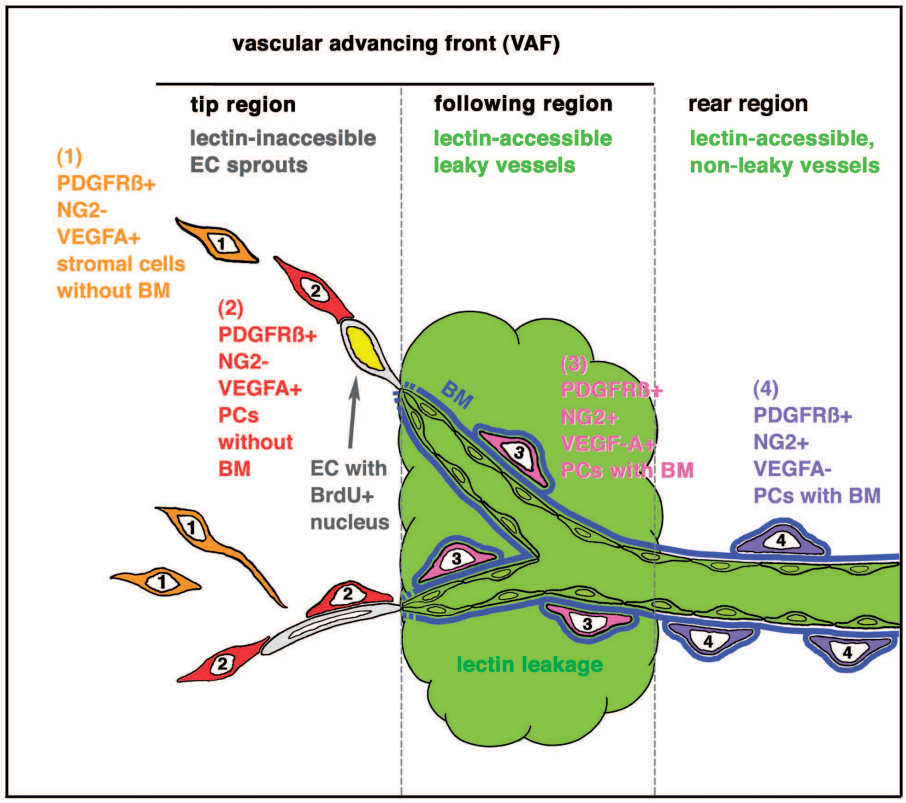

Fig. 10: Schematic drawing showing the distribution and phenotypic features of PCs in the regenerating vessels of a Day 5 wound. (1) PDGFR+/NG2- stromal cells that were out of contact with ECs were observed in the tip region of vascular advancing front (VAF); they expressed VEGF-A, and often seemed to approach ECs by sprawling their cytoplasmic processes. (2) In the tip region, PCs with similar phenotypes to the stromal cells described in (1) were predominant: These were positive for PDGFR-ß but negative for NG2, usually lacked a BM coating, expressed VEGF-A, and were associated with lectin-inaccessible EC sprouts. (3) The following region of the VAF was located behind the tip region and characterized by the distribution of lectin-accessible but leaky vessels. In this region, PDGFR-ß+/NG2+ PCs predominated in turn. They were usually covered with a BM in common with ECs and expressed VEGF-A. (4) In the vessels located toward the rear of VAF, lectin leakage was no longer observed. PDGFR-ß+/NG2+ PCs with a BM coating were distributed in this region, although they no longer expressed VEGF-A.

associated with EC sprouts (Fig. 9A). Together, these ultrastructural findings correspond well with the immunohistochemical observations shown in Fig. 6, in which PDGFR-ß+ PCs were situated on the BrdU-labelled proliferating ECs in the tip region. Around sprouts, vascular BM detectable on the vessel surface disappeared at the root of sprouts (Fig. 9B). Vascular BM was also not detectable on associating PCs (Fig. 9C). Similar to other PCs, the PCs on sprouts were rich in rER (Fig. 9C); well-developed Golgi areas were also noticeable (Fig. 9C). Similar to PCs, stromal cells distributed in close proximity of EC sprouts also contained abundant rER (Fig. 9A).

Discussion

The aim of this study was to determine whether PCs vary in their phenotypes and functional roles depending on the stage of angiogenesis. The functional role of PCs during angiogenesis has not been strictly elucidated so far, despite the fact that it is crucial for a comprehensive understanding of the angiogenic mechanism. Their role remains enigmatic because two conflicting functions, namely, inhibition and promotion of EC proliferation, have been simultaneously proposed as functions of PCs during angiogenesis. We hypothesized that these conflicting roles might reflect two different aspects of this cell type, and that PCs might be heterogenic in their phenotypes or functional roles in the different stages (initial or later maturing stage) of angiogenesis. To verify our hypothesis, we prepared a wound-healing model in which the different stages of angiogenesis were identifiable. Then we visualized PCs within that model using PC specific markers, and examined their phenotypes in the different angiogenic stages. We employed two markers, PDGFR-ß and NG2, for PC identification. These markers have been recognized as specific markers for PCs, especially in the process of angiogenesis and vasculogenesis (Hellstrom et al., 1999; Bergers and Song, 2005; Hall, 2006).

Time course of angiogenesis during wound healing

A dynamic angiogenic process was clearly visualized through the examination of tomato lectin-perfused skin vasculature in whole-mount specimens. Tomato lectin is a glycoprotein of 71 kD that binds to N-acetylglucosamines on EC surfaces. In this study, extravasation of lectin was observed during wound healing. The amount of extravasated lectin became conspicuous and the pools of leaked lectin formed a clear circular structure in the VAF of regenerating vessels. The circular structure of leaked lectin closely resembled the structure described by Cliff (1963), who examined angiogenesis in rabbit ear chambers, and named the zone of hemorrhage at the leading edge of the regenerating vessels the "vascular growing fringe."

Newly formed vessels are characterized by their increased permeability, and VEGF-A, also known as vascular permeability factor (VPF) (Dvorak, 2006), presumably makes an important contribution to this state since an intense expression of VEGF-A was observed in VAF of regenerating vessels.

Lectin leakage was first observed on Day 3, and became conspicuous on Day 5. By Day 10, vessels were totally connected and formed an organized circulation. The time course of angiogenesis observed in the skin wound was compatible to that of wounds in skeletal muscles (Schoefl, 1964), suggesting that the time span of angiogenic reaction is fairly constant regardless of wound type. Therefore, we chose the healing process on Day 5 for more detailed examination.

Phenotypic changes of PCs according to the regions (stages) of angiogenesis

The regenerating vessel network was first divided into VAF and a region rear the VAF. The VAF appeared to be composed of immature vessels, and was further divided into two regions based on the accessibility of perfused lectin: the tip and following regions. These specific regions of the regenerating vessels were considered to represent sequential but different stages of angiogenesis; that is, the degree of maturation of the regenerating vessels gradually increased from the tip toward the rear. PCs were found constantly in the regenerating vessels of the VAF, and the ratios of their association with BrdU+ ECs were almost the same in the tip and following regions. Notably, PCs identified in regenerating vessels changed their phenotypes from the tip of the VAF toward the rear and their phenotypic features in each region are summarized in Fig. 10.

In the tip region of the VAF, (1) stromal cells that were out of contact with ECs but that expressed marker PDGFR-ß were identified. These were negative for another PC marker NG2, typically lacked a vascular BM coat, expressed VEGF-A, and often approached EC surfaces to attach to these surfaces with their cytoplasmic processes. (2) PCs with a similar expression pattern of markers (PDGFR-ß+/NG2-/VEGF-A+) were predominantly associated with most BrdU+ ECs and sprouting ECs in this region. They also did not have a BM coating. (3) In the following region, PCs positive for both PC markers (PDGFR-ß+/NG2+) became predominant. In contrast to PCs in the tip region, these were covered with a BM in common with the ECs. These ECs also expressed VEGF-A. (4) In the rear of the VAF, PDGFR-ß+/NG2+ PCs with a BM coating were successively seen, but these PCs lost their VEGF-A expression.

Relation of different PC phenotypes to their recruitment to the VAF

The phenotypic changes in PCs in the different regions (different angiogenic stages) were presumably correlated with the recruitment and differentiation of PCs from the mesenchyme for angiogenesis: During

wound healing, a large amount of skin tissue, including the vasculature, is removed, and thus a number of PCs have to be newly recruited to the cut end of the blood vessels for their regeneration. It is generally accepted that the interaction between PDGFR-ß and its ligand, platelet-derived growth factor B (PDGF-B), is a significant pathway for the recruitment of PCs to ECs during vasculogenesis and angiogenesis (Lindahl et al., 1997; Armulik et al., 2005; Bergers and Song, 2005; Hall, 2006). In this signaling pathway, PDGFR-ß expressing PC precursors are attracted by PDGF-B expressed by ECs, and the blockade of this signaling pathway leads to a lack of PCs and eventually to abnormal vessel formation (Lindahl et al., 1997). Thus, PDGFR-ß+/NG2- stromal cells distributed in the tip region might be PC precursors from the mesenchyme, and the PCs with similar PC marker expression could represent the former PC precursors that have by this stage attached to EC surfaces. Accordingly, the differentiation of mesenchymal cells into PCs has long been well documented using electron microscopy (Crocker et al., 1970; Rhodin and Fujita, 1989; Nehls and Drenckhahn, 1993), autoradiography (Cavallo et al., 1972; Diaz-Flores et al., 1991), and cell-transplantation techniques (Xueyong et al., 2008). Newly recruited PCs might express NG2 as the next step. The presence of PCs with uniform PDGFR-ß and partial NG2 expression in the tip region might thus represent newly recruited PCs that are going through the process of acquiring NG2 expression. The existence of PCs with and without BM also suggests their recruitment from outside the vessel wall. The terms "intramural" and "extramural" PCs were first introduced by Ashton and de Oliveira (1966). The former designates PCs situated within the vascular BM on vessels, while the latter designates those situated beyond. Normally, PCs are situated in their intramural position; they are situated outside under special conditions, such as during development (Ashton and de Oliveira, 1966; Nehls and Drenckhahn, 1993; Gerhardt and Betsholtz, 2003). Immunohistochemical and ultrastructural studies confirmed that PCs in the tip region typically lacked vascular BM and appeared to be extramural. This finding suggests that PCs in this region are in a state that where they have been differentiated from precursor cells in the mesenchyme and have landed on EC surfaces, but have not yet been encapsulated into the vascular BM of the regenerating vessels. Coincidentally, ultrastructural studies using a hamster wound model (Crocker et al., 1970) and a rat inflammation model (Rhodin and Fujita, 1989) have suggested that extramural PCs recruited from the mesenchyme are gradually encapsulated within the vascular BM. Since the production of BM components such as laminin and type-IV collagen by PCs has also been suggested (Jeon et al., 1996), these extramural PCs might themselves promote encapsulation by producing a new vascular BM for themselves.

These extramural PCs likely originate from precursors that come from bone marrow via the blood stream (Rajantie et al., 2004; Ozerdem et al., 2005; Diaz-Flores Jr. et al., 2006; Xueyong et al., 2008; Diaz-Flores et al., 2009). Indeed, Ozerdem et al. (2005) reported that more than half of the PCs found at sites of revascularization in corneal angiogenesis were recruited from bone marrow. The authors also reported that remaining PC population was derived from local pre-existing vessels. It has been well documented that during angiogenesis, pre-existing PCs are activated and leave their original location to become PC precursors (Diaz-Flores et al., 1991, 1992, 2009; Diaz-Flores Jr. et al., 2006). Thus, pre-existing PCs are also candidates for the source of these extramural PCs.

Some PCs also contain cytoskeletal proteins α-SMA and desmin (Kurz et al., 2002, 2008). In our wound-healing model, we were also able to detect these proteins of PCs located in the regenerating vessels. Intriguingly, we observed that α-SMA and desmin also marked additional PDGFR-ß-expressing stromal cells. Since stromal cells with α-SMA and desmin expression are classified as a type of myofibroblasts (Badid et al, 2000; Gabbiani, 2003), these stromal cells might be a subpopulation of myofibroblasts. Myofibroblasts are known to play major roles in wound healing process, such as constricting the wound tissue, and producing extracellular matrix (Badid et al, 2000; Gabbiani, 2003). Co-localization of α-SMA, desmin, and PDGFR-ß in stromal cells may therefore suggest a further possible role of myofibroblasts as precursors of PCs (Diaz-Flores et al., 2009).

Phenotypic differences in PCs presumably reflect their different functions in each location (each angiogenic stage), as discussed below.

Functions of PCs in the tip region of the VAF

Blood vessels in the tip region were characterized by their inaccessibility to intravascular lectin (Fig. 10). This lectin inaccessibility was presumably due to the presence of solid EC sprouts from blood vessels that were CD31+ but had no luminal surfaces. Notably, many BrdU+ ECs, presumably representing their proliferative state, were also identified in this region. Moreover, these EC sprouts and BrdU+ ECs were mostly associated with PCs. Thus, PCs in this region are likely to induce EC proliferation and guide their sprouting. The close topographical relationship between PCs and ECs may permit a precise regulation of individual EC proliferation and migration. PC association with lectin-inaccessible EC sprouts has also been identified previously in tumor vessels, and PCs have also been suggested to have a role in guiding ECs (Morikawa et al., 2002). A similar hypothesis has been proposed for angiogenesis of ovarian corpuscles (Reynolds and Redmer, 1998; Amselgruber et al., 1999; Reynolds et al., 2000) and inflammation (Nehls and Drenckhahn, 1993). This guidance hypothesis is supported by another finding from this study that PCs in this region express an important EC growth factor VEGF-A, which is known to be a key factor in the

proliferation and migration of ECs during angiogenesis (Ferrara, 2004; Gerhardt et al., 2003). VEGF-A expression by PCs was restricted to the VAF of regenerating vessels, and was not observed in the vessels in the rear of the VAF or in control normal skin (data not shown). PCs in this region were ultrastructurally characterized by a large amount of rER, suggesting their increased synthesis of proteins such as VEGF-A. In our preliminary experiments, we confirmed that PCs in control normal skin or in the rear of the VAF contain only a moderate amount of rER, which is also a common feature of normal PCs (Diaz-Flores et al., 1991, 2009; Sims, 2000). VEGF-A production by PCs has also been reported by several studies on angiogenic processes other than wound healing (Reynolds et al., 2000; Reinmuth et al., 2001; Darland et al., 2003), and by myofibroblasts during wound healing (Staton et al, 2010).

The tip region of the VAF is defined as the region for de novo production of vessels, representing the initial stage of angiogenesis, and PCs may make an important contribution to the production of new vessels via VEGF-A secretion. To our knowledge, our study provides the first comprehensive demonstration of the facilitating role of PCs in the initial stage of angiogenesis. Interestingly, elongation and migration of PCs under the influence of VEGF-A has been suggested in experimental angiogenesis of chicken chorioallantic membrane (Hagedorn et al, 2004). VEGF-A secreted by PCs and stromal cells might thus act not only upon ECs, but also on PCs and stromal cells themselves, via VEGF-A autocrine/paracrine signaling, enabling these cells to migrate.

Functions of PCs in other parts of the VAF

The following region consists of the posterior region of the vascular advancing front that was characterized by an abundance of lectin-accessible but leaky vessels (Fig. 10). These vessels can function as blood channels and their continuous BM coating indicates some degree of maturity, although their high permeability shows that they are still not fully stabilized. This region may be defined as a transitional region between immature and mature vessels. Although PCs in this region were phenotypically different in terms of their NG2 expression, some of their activated characteristics were common to the PCs at the tip region. For example, PCs in the following region express VEGF-A, which might be necessary for subsequent vessel remodelling following the initial vessel sprouting and migration that occurred in the tip region. Accordingly, proliferating ECs were still found in this region, although they were far fewer in number compared with the tip region.

Lectin leakage disappeared in the rear of the VAF, suggesting the maturation of vessels in this area. Coincidentally, PCs in this region lacked VEGF-A expression. They might stabilize the vessels in this region: Transforming growth factor-ß (TGF-ß) is known to serve as a stabilizer for vessel walls (Gaengel et al., 2009), and NG2 can indirectly activate latent TGF-ß (Ozerdem et al., 2001). Thus, PCs might stabilize the vessel wall by increasing the level of TGF-ß in this region. The stabilization might be performed effectively in environments where VEGF-A is absent.

Conclusions

Pericytes differ phenotypically in the different stages of angiogenesis during wound healing. We conclude that pericytes are likely to facilitate EC proliferation and migration via secretion of VEGF-A, especially in the initial stages of angiogenesis, but during the later stages they gradually change their phenotype to stabilize the newly formed blood vessels.

In addition to PCs, involvement of macrophages in neovascularization has been reported (Cossmann et al., 1997; Rodero and Khosrotehrani, 2010). For the comprehensive understanding of angiogenic mechanism, further studies concerning macrophages are needed in the next step.

Acknowledgments. We thank Prof. D.M. McDonald and Dr. P. Baluk (Cardiovascular Research Institute, University of California, San Francisco, USA) for their valuable suggestions on the manuscript and their encouragement. We also thank Ms. Y. Yamazaki for her excellent technical support. This study was supported in part by a Grant-in-Aid for Scientific Research (#20590199) from the Japan Society for the Promotion of Science.

References

Amselgruber W.M., Schafer M. and Sinowatz F. (1999). Angiogenesis in the bovine corpus luteum: an immunocytochemical and ultrastructural study. Anat. Histol. Embryol. 28, 157-166.

Armulik A., Abramsson A. and Betsholtz C. (2005). Endothelial/pericyte interactions. Circ. Res. 97, 512-523.

Ashton N. and de Oliveira F. (1966). Nomenclature of pericytes. Intramural and extramural. Br. J. Ophthalmol. 50, 119-123.

Badid C., Mounier N., Costa A.M. and Desmouliere A. (2000) Role of myofibroblasts during normal tissue repair and excessive scarring: interest of their assessment in nephropathies. Histol. Histopathol. 15, 269-280.

Baluk P., Hashizume H. and McDonald D.M. (2005). Cellular abnormalities of blood vessels as targets in cancer. Curr. Opin. Genet. Dev. 15, 102-111.

Bergers G. and Song S. (2005). The role of pericytes in blood-vessel formation and maintenance. Neuro-Oncol. 7, 452-464.

Cavallo T., Sade R., Folkman J. and Cotran R.S. (1972). Tumor angiogenesis. Rapid induction of endothelial mitoses demonstrated by autoradiography. J. Cell Biol. 54, 408-420.

Cliff W.J. (1963). Observations on healing tissue: A combined light and electron microscopic investigation. Phil. Trans. R. Soc. B 246, 305-325.

Cossmann P.H., Eggli P.S., Christ B. and Kurz H. (1997). Mesoderm-derived cells proliferate in the embryonic central nervous system: confocal microscopy and three-dimensional visualization.

Histochem. Cell Biol. 107, 205-213.

Crocker D.J., Murad T.M. and Geer J.C. (1970). Role of the pericyte in wound healing. An ultrastructural study. Exp. Mol. Pathol. 13, 51-65.

Darland D.C., Massingham L.J., Smith S.R., Piek E., Saint-Geniez M. and D'Amore P.A. (2003). Pericyte production of cell-associated VEGF is differentiation-dependent and is associated with endothelial survival. Dev. Biol. 264, 275-288.

Diaz-Flores L., Gutierrez R., Varela H., Rancel N. and Valladares F. (1991). Microvascular pericytes: a review of their morphological and functional characteristics. Histol. Histopathol. 6, 269-286.

Diaz-Flores L., Gutierrez R. and Varela H. (1992). Behavior of postcapillary venule pericytes during postnatal angiogenesis. J. Morphol. 213, 33-45.

Diaz-Flores L. Jr., Madrid J.F., Gutierrez R., Varela H., Valladares F., Alvarez-Arguelles H. and Diaz-Flores L. (2006). Adult stem and transit-amplifying cell location. Histol. Histopathol. 21, 995-1027.

Diaz-Flores L., Gutierrez R., Madrid J.F., Varela H., Valladares F., Acosta E., Martin-Vasallo P. and Diaz-Flores L. Jr. (2009). Pericytes. Morphofunction, interactions and pathology in a quiescent and activated mesenchymal cell niche. Histol. Histopathol. 24, 909-969.

Dvorak H.F. (2006). Discovery of vascular permeability factor (VPF). Exp. Cell Res. 312, 522-526.

Erber R., Thurnher A., Katsen A.D., Groth G., Kerger H., Hammes H.P., Menger M.D., Ullrich A. and Vajkoczy P. (2004). Combined inhibition of VEGF and PDGF signaling enforces tumor vessel regression by interfering with pericyte-mediated endothelial cell survival mechanisms. FASEB J. 18, 338-340.

Ezaki T., Baluk P., Thurston G., La Barbara A., Woo C., and McDonald D.M. (2001). Time Course of Endothelial Cell Proliferation and Microvascular Remodeling in Chronic Inflammation. Am. J. Pathol. 158, 2043-2055.

Ferrara N. (2004). Vascular endothelial growth factor: basic science and clinical progress. Endocr. Rev. 25, 581-611.

Gabbiani G. (2003). The myofibroblast in wound healing and fibrocontractive diseases. J. Pathol. 200, 500-503.

Gaengel K., Genove G., Armulik A. and Betsholtz C. (2009). Endothelial-mural cell signaling in vascular development and angiogenesis. Arterioscler. Thromb. Vasc. Biol. 29, 630-638.

Gerhardt H. and Betsholtz C. (2003). Endothelial-pericyte interactions in angiogenesis. Cell Tissue Res. 314, 15-23.

Gerhardt H., Golding M., Fruttiger M., Ruhrberg C., Lundkvist A., Abramsson A., Jeltsch M., Mitchell C., Alitalo K., Shima D. and Betsholtz C. (2003). VEGF guides angiogenic sprouting utilizing endothelial tip cell filopodia. J. Cell Biol. 161, 1163-1177.

Hagedorn M., Balke M., Schmidt A., Bloch W., Kurz H., Javerzat S., Rousseau B., Wilting J. and Bikfalvi A. (2004). VEGF coordinates interaction of pericytes and endothelial cells during vasculogenesis and experimental angiogenesis. Dev. Dyn. 230, 23-33.

Hall A.P. (2006). Review of the pericyte during angiogenesis and its role in cancer and diabetic retinopathy. Toxicol. Pathol. 34, 763-775.

Hellstrom M., Kalen M., Lindahl P., Abramsson A. and Betsholtz C. (1999). Role of PDGF-B and PDGFR-beta in recruitment of vascular smooth muscle cells and pericytes during embryonic blood vessel formation in the mouse. Development 126, 3047-3055.

Jeon H., Ono M., Kumagai C., Miki K., Morita A. and Kitagawa Y. (1996). Pericytes from microvessel fragment produce type IV collagen and multiple laminin isoforms. Biosci. Biotechnol. Biochem. 60, 856-861.

Kurz H., Lauer D., Papoutsi M., Christ B. and Wilting J. (2002). Pericytes in experimental MDA-MB231 tumor angiogenesis. Histochem. Cell Biol. 117, 527-534.

Kurz H., Fehr J., Nitschke R. and Burkhardt H. (2008). Pericytes in the mature chorioallantoic membrane capillary plexus contain desmin and alpha-smooth muscle actin: relevance for non-sprouting angiogenesis. Histochem. Cell Biol. 130, 1027-1040.

Lindahl P., Johansson B.R., Leveen P. and Betsholtz C. (1997). Pericyte loss and microaneurysm formation in PDGF-B-deficient mice. Science 277, 242-245.

Morikawa S., Baluk P., Kaidoh T., Haskell A., Jain R.K. and McDonald D.M. (2002). Abnormalities in pericytes on blood vessels and endothelial sprouts in tumors. Am. J. Pathol. 160, 985-1000.

Nehls V., Denzer K. and Drenckhahn D. (1992). Pericyte involvement in capillary sprouting during angiogenesis in situ. Cell Tissue Res. 270, 469-474.

Nehls V. and Drenckhahn D. (1993). The versatility of microvascular pericytes: from mesenchyme to smooth muscle? Histochemistry 99, 1-12.

Orlidge A. and D'Amore P.A. (1987). Inhibition of capillary endothelial cell growth by pericytes and smooth muscle cells. J. Cell Biol. 105, 1455-1462.

Ozerdem U., Grako K.A., Dahlin-Huppe K., Monosov E. and Stallcup W.B. (2001). NG2 proteoglycan is expressed exclusively by mural cells during vascular morphogenesis. Dev. Dyn. 222, 218-227.

Ozerdem U. and Stallcup W.B. (2003). Early contribution of pericytes to angiogenic sprouting and tube formation. Angiogenesis 6, 241-249.

Ozerdem U., Alitalo K., Salven P. and Li A. (2005). Contribution of bone marrow-derived pericyte precursor cells to corneal vasculogenesis. Invest. Ophthalmol. Vis. Sci. 46, 3502-3506.

Rajantie I., Ilmonen M., Alminaite A., Ozerdem U., Alitalo K. and Salven P. (2004). Adult bone marrow-derived cells recruited during angiogenesis comprise precursors for periendothelial vascular mural cells. Blood 104, 2084-2086.

Reinmuth N., Liu W., Jung Y.D., Ahmad S.A., Shaheen R.M., Fan F., Bucana C.D., McMahon G., Gallick G.E. and Ellis L.M. (2001). Induction of VEGF in perivascular cells defines a potential paracrine mechanism for endothelial cell survival. FASEB J. 15, 1239-1241.

Reynolds L.P. and Redmer D.A. (1998). Expression of the angiogenic factors, basic fibroblast growth factor and vascular endothelial growth factor, in the ovary. J. Anim. Sci. 76, 1671-1681.

Reynolds L.P., Grazul-Bilska A.T. and Redmer D.A. (2000). Angiogenesis in the corpus luteum. Endocrine 12, 1-9.

Rhodin J.A. and Fujita H. (1989). Capillary growth in the mesentery of normal young rats. Intravital video and electron microscope analyses. J. Submicrosc. Cytol. Pathol. 21, 1-34.

Rodero M.P. and Khosrotehrani K. (2010). Skin wound healing modulation by macrophages. Int. J. Clin. Exp. Pathol. 3, 643-653.

Sato Y. and Rifkin D.B. (1989). Inhibition of endothelial cell movement by pericytes and smooth muscle cells: activation of a latent transforming growth factor-beta 1-like molecule by plasmin during co-culture. J. Cell Biol. 109, 309-315.

Schlingemann R.O., Rietveld F.J., Kwaspen F., van de Kerkhof P.C., de Waal R.M. and Ruiter D.J. (1991). Differential expression of markers for endothelial cells, pericytes, and basal lamina in the microvasculature of tumors and granulation tissue. Am. J. Pathol. 138, 1335-1347.

Schoefl G.I. (1964). Electron microscopic observations on the regeneration of blood vessels after Injury. Ann. N. Y. Acad. Sci. 116, 789-802.

Sennino B., Falcon B.L., McCauley D., Le T., McCauley T., Kurz J.C., Haskell A., Epstein D.M. and McDonald D.M. (2007). Sequential loss of tumor vessel pericytes and endothelial cells after inhibition of platelet-derived growth factor B by selective aptamer AX102. Cancer Res. 67, 7358-7367.

Sennino B., Kuhnert F., Tabruyn S.P., Mancuso M.R., Hu-Lowe D.D., Kuo C.J. and McDonald D.M. (2009). Cellular source and amount of vascular endothelial growth factor and platelet-derived growth factor in tumors determine response to angiogenesis inhibitors. Cancer Res. 69, 4527-4536.

Sims D.E. (2000). Diversity within pericytes. Clin. Exp. Pharmacol. Physiol. 27, 842-846.

von Tell D., Armulik A. and Betsholtz C. (2006). Pericytes and vascular stability. Exp. Cell Res. 312, 623-629.

Staton C.A., Valluru M., Hoh L., Reed M.W. and Brown N.J. (2010). Angiopoietin-1, angiopoietin-2 and Tie-2 receptor expression in human dermal wound repair and scarring. Br. J. Dermatol. 163, 920-927.

Wesseling P., Schlingemann R.O., Rietveld F.J., Link M., Burger P.C. and Ruiter D.J. (1995). Early and extensive contribution of pericytes/vascular smooth muscle cells to microvascular proliferation in glioblastoma multiforme: an immuno-light and immuno-electron microscopic study. J. Neuropathol. Exp. Neurol. 54, 304-310.

Xueyong L., Shaozong C., Wangzhou L., Yuejun L., Xiaoxing L., Jing L., Yanli W. and Jinqing L. (2008). Differentiation of the pericyte in wound healing: The precursor, the process, and the role of the vascular endothelial cell. Wound Repair Regen. 16, 346-355.

Accepted February 4, 2011